PERGAMON

Applied Geochemistry 14 (1999) 1015–1030

Applied Geochemistry

Mineralogy and geochemistry of alluvium contaminated by metal mining in the Rio Tinto area, southwest Spain

Karen A. Hudson-Edwards[a,*,1], Christiane Schell[b], Mark G. Macklin[b]

[a]*Department of Earth Sciences, University of Manchester, Manchester M13 9PL, UK*
[b]*School of Geography, University of Leeds, Leeds LS2 9JT, UK*

Received 27 January 1998; accepted 7 January 1999
Editorial handling by O. Selinus

Abstract

The Rio Tinto in SW Spain drains Cu and pyrite mines which have been in operation since at least the Bronze Age. Extensive metal mining, especially from 1873 to 1954, has resulted in contamination of the Rio Tinto alluvium with As, Cu, Pb, Ag and Zn. X-ray diffraction (XRD), wavelength-dispersive X-ray mapping, scanning electron microscope petrography and X-ray energy-dispersive (EDX) analysis has revealed that 4 major groups of contaminant metal and As-bearing minerals, including sulphides, Fe-As oxides, Fe oxides/hydroxides/oxyhydroxides, and Fe oxyhydroxysulphates, occur in the alluvium. Sulphide minerals, including pyrite, chalcopyrite, arsenopyrite and sphalerite, occur in alluvium near the mining areas. Iron hydroxides and oxyhydroxides such as goethite and possibly ferrihydrite occur in cements in both the mining areas and alluvium downstream, and carry minor amounts of As, Cu and Zn. Iron oxyhydroxysulphates, including jarosite, plumbojarosite and possibly schwertmannite, are the most common minerals in alluvium downstream of the mining areas, and are major hosts of Cu, Pb, Zn and of As, next to the Fe-As minerals. This work, and other field observations, suggest that (1) the extreme acidity and elevated metal concentrations of the river water will probably be maintained for some time due to oxidation of pyrite and other sulphides in the alluvium and mine-waste tips, and from formation of secondary oxide and oxyhydroxysulphates; (2) soluble Fe oxyhydroxysulphates such as copiapite, which form on the alluvium, are a temporary store of contaminant metals, but are dissolved during periods of high rainfall or flooding, releasing contaminants to the aqueous system; (3) relatively insoluble Fe oxyhydroxysulphates and hydroxides such as jarosite and goethite may be the major long-term store of alluvial contaminant metals; and (4) raising river pH will probably cause precipitation of Fe oxyhydroxides and oxides/hydroxides/oxyhydroxides and thus have a positive effect on water quality, but this action may destabilise some of these contaminant metal-bearing minerals, releasing metals back to the aqueous system.

* Corresponding author.
E-mail address: k.hudson-edwards@geology.bbk.ac.uk (K.A. Hudson-Edwards)
[1] Now at Department of Geology, Birkbeck College, University of London, London WC1E 7HX, UK.

1. Introduction

Rivers draining both operating and abandoned sulphide ore mines are often seriously affected by acid

0883-2927/99/$ - see front matter
PII: S0883-2927(99)00008-6

run-off from mine workings and tailings, and waste rock piles (e.g., Filipek et al., 1987; Boult et al., 1994). Although oxidation of sulphide minerals (particularly pyrite) results in the discharge of considerable quantities of metal ions to river waters (Nordstrom, 1977, 1982; Fuge et al., 1993), a large proportion of the metal is stored in Fe ochres which flocculate and adsorb metal cations (Langmuir and Whittemore, 1971; Nordstrom, 1982; Chapman et al., 1983; Johnson, 1986). These ochres, and mobilised metal-bearing tailings and waste, can be stored in alluvial sediment for considerable periods of time (tens to thousands of years), and constitute a long-term threat to river and agricultural quality (Salomons and Förstner, 1984; Macklin, 1996).

The Rio Tinto in SW Spain is an acid mine drainage river (Garcia-Vargas et al., 1980). Extensive study has shown that both water (Garcia-Vargas et al., 1979, 1980; Boyle et al., 1988; van Geen et al., 1988, 1990, 1991, 1997; van Geen and Boyle, 1990; López-Archilla et al., 1993; Nelson and Lamothe, 1993; Leblanc et al., 1995; Elbaz-Poulichet and Leblanc, 1996; Muñoz et al., 1997) and fluvial and estuarine sediment quality have been seriously affected by the mining activity (Nelson and Lamothe, 1993; Welty et al., 1995; Schell et al., 1996; van Geen et al., 1997), and that much of this contamination took place during the past 125 a (Strauss et al., 1977; Harvey, 1981). Due to growing concern about these environmental impacts, remediation strategies are currently being considered by regional authorities. Knowledge of the forms of sediment-borne metal present in contaminated sediments and soils is critical in developing such strategies (e.g., Davis et al., 1993; Ruby et al., 1994). In the Rio Tinto area, however, little mineralogical work, apart from that on the orebodies (Williams, 1950; Pryor et al., 1972; Amorós et al., 1981; Dutrizac et al., 1983), has been attempted. The objectives of this paper are thus to (1) characterise the mineralogy of alluvial sediments; (2) infer chemical reactions occurring in the mine-waste tips, river water and alluvium; and (3) make predictions about alluvial mineral stability under changing environmental conditions. For simplicity, the term 'contaminant metal' is used in this paper to refer collectively to Ag, Cu, Pb, Zn *and* As.

2. The Rio Tinto mining district

The Rio Tinto in SW Spain drains the world's oldest continuously operating mine (Wilson, 1981). The Rio Tinto mining district is part of the Iberian Pyrite Belt (Fig. 1) that extends for 230 km NW of Seville into Portugal (Williams et al., 1975; Schermerhorn, 1982; Munha et al., 1986). The area is underlain by the Lower Carboniferous Volcanic-Sedimentary Complex, a series of slates, shales and acid and basic volcanic rocks which host massive and stockwork pyrite orebodies containing other base and precious metals such as Cu, Pb, Zn, Au and Ag. These orebodies are generally capped by a gossan or 'iron hat' (Dutrizac et al., 1983), which averages about 30 m in thickness, is flat-lying, has a sharp contact with the underlying massive pyrite, and is composed predominantly of goethite and hematite. Near the base of the gossan, a jarositic layer ranging in thickness from a few centimetres to 1.5 m thick is often present (Williams, 1934, 1950). Mineralogically this comprises quartz, Fe oxides, baryte, cerussite, anglesite, scorodite and a variety of minerals from the jarosite family including plumbojarosite, argentojarosite, natrojarosite and jarosite (Table 1, Williams, 1950, Pryor et al., 1972, Amorós et al., 1981, Dutrizac et al., 1983).

Mining for Cu, Au, Ag and pyrite has been carried out, using both opencast and underground mining methods, from approximately 2500 B.C. to the present day (Pinedo, 1963; Strauss et al., 1977) during which time approximately 115 million tonnes of ore have been extracted (Badham, 1982; Schermerhorn, 1982). At least 90% of this production took place between the mid-nineteenth century and the 1970s (Strauss et al., 1977). The ores contain on average 50% S, 42% Fe, 2–8% Cu, Pb and Zn, and significant quantities of Au and Ag (Strauss et al., 1977). Mining of the jarositic layer for Ag began as early as 1200 B.C. (Jones, 1982; Morral, 1990) and continued to the early Roman period, by which time two million tons had been extracted (Dutrizac et al., 1983). Gold and Ag are still being mined in the area.

3. Methodology

Samples of alluvial sediment and mine-waste tips and tailings were collected using a stainless steel trowel and stored in air-tight bags. Alluvial sediment and mine-waste and tailings tips samples were collected both from surfaces of, and up to 0.5 m deep within, the units (Table 2). Mineral precipitates on the surfaces of alluvial sediment were collected using a stainless steel spatula and stored in air-tight glass vials. Two separate water samples were collected at each site: one was filtered through a 0.45 μm Millipore filter and acidified with 1 M HNO_3 and the other was collected unprocessed. The water samples were stored in acid-washed, air-tight glass bottles. Redox potential, pH, temperature and conductivity were measured using a Hanna Instruments water tester, calibrated with the standards supplied. Duplicate water samples were filtered in the laboratory after standing for one week, and the filtered precipitate was both mounted on slides, gold-coated and examined under the scanning

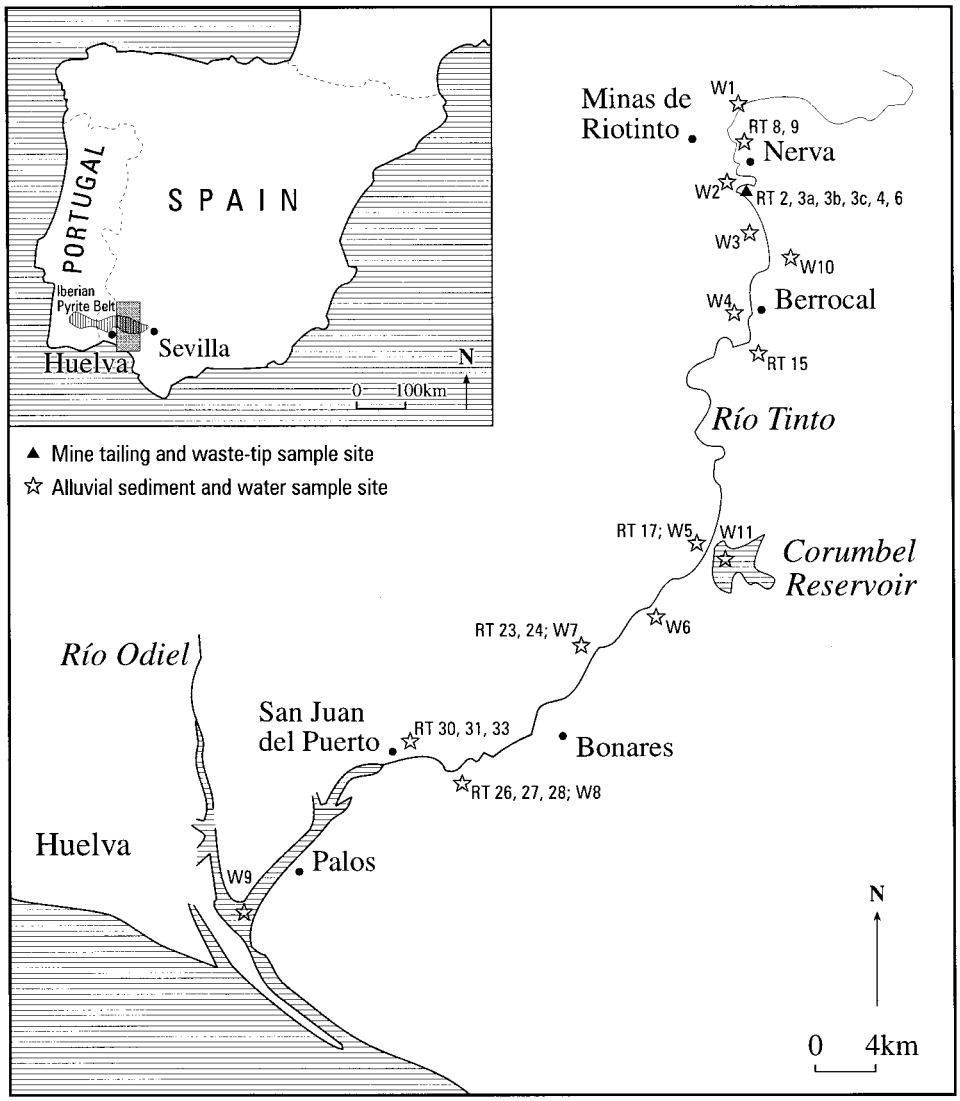

Fig. 1. Location map of the Rio Tinto study area, showing the sites of sediment and water sampling.

electron microscope and by X-ray diffraction (see below).

Mineral identification was carried out by optical and electron microscopy (Jeol JSM 6400 scanning electron microscope (SEM) combined with energy dispersive X-ray spectrometry (EDX) and equipped with a Link Analytical backscattered electron detector; Cameca CAMEBAX electron microprobe) and confirmed in many cases by X-ray diffraction (Philips PW1730 instrument with Cu (Kα) radiation at 40 kV/20 Ma operating conditions). Operating conditions for the SEM were 15 kV accelerating voltage and 1.5 nA incident specimen current. Analytical data were obtained on the SEM using a standardless Link Analytical eXL energy dispersive analysis system with a ZAF4–FLS deconvolution/recalculation package. Counting time was 45 s for each analysis. X-ray element mapping for Fe, S, Pb, As, Cu and Zn was performed on the Cameca microprobe using the Oxford Instruments (Link Analytical) SPECTA software. Operating conditions were 20 to 30 kV accelerating voltage depending on the elements analysed, and 15 nA incident specimen current. Magnifications of 200 to 800, and dwell times of 50 to 700 ms were used. Attempts were made to map Ag but only background patterns were obtained.

Trace elements were extracted from the sediment using a HNO_3 digestion procedure (cf. Harrison and Laxen, 1981). Approximately 1 g of sample was accurately weighed into a 250 mL beaker. Ten mL of

Table 1
Minerals described from the Rio Tinto mines and river, Spain (Calderón, 1910; Galan and Mirete, 1979; Amorós et al., 1981; Dutrizac et al., 1983; García, 1996; this study). Minerals highlighted in bold occur, or are inferred to occur, in the alluvial sediments described in this study. "Contaminant metal-bearing group" refers to the 4 types of contaminant metal-bearing minerals discussed in this paper, including sulphides, Fe-As oxides (designated Fe–As–O), Fe oxides/hydroxides/oxyhydroxides (designated Fe–O), or Fe oxyhydroxysulphates (designated Fe–S–O). Primary (P) contaminant metal-bearing minerals include detrital minerals from the orebody, waste tips and gossan, and secondary (S) minerals include those in cements, overgrowths on other primary or secondary minerals, and precipitates on alluvium

Mineral	Formula	Contaminant metal-bearing group	Primary (P)/ Secondary (S)
Alunogen	$Al_2(SO_4)_3{\cdot}17H_2O$		
Anglesite	$PbSO_4$		
Argentopyrite	$AgFe_2S_3$		
Argentojarosite	$AgFe_3(SO_4)_2(OH)_6$	Fe–S–O	P
Arsenopyrite	FeAsS	Sulphide	P
Azurite	$Cu_3(CO_3)_2(OH)_2$		
Baryte	$BaSO_4$		
Beaverite	$Pb(Fe,Cu)_3(SO_4)_2(OH)_6$	Fe–S–O	P, S
Bornite	Cu_5FeS_4		
Botryogen	$MgFe(SO_4)_2(OH){\cdot}7H_2O$		
Cerargyrite	AgCl		
Cerussite	$PbCO_3$		
Chalcanthite	$CuSO_4{\cdot}5H_2O$		
Chalcocite	Cu_2S		
Chalcopyrite	$CuFeS_2$	Sulphide	P
Chlorite	$(Mg,Fe,Al)_6(Si,Al)_4O_{10}(OH)_8$		
Copiapite	$Fe^{2+}Fe_4^{3+}(SO_4)_6(OH)_2{\cdot}20H_2O$	Fe–S–O	S
Copper	Cu		
Cuprite	CuO		
Coquimbite	$Fe_2^{3+}(SO_4)_3{\cdot}9H_2O$	Fe–S–O	S
Covellite	CuS		
Epsomite	$MgSO_4{\cdot}7H_2O$		
Ferrihydrite	$Fe_2O_3{\cdot}2H_2O$	Fe–O	S
Galena	PbS	Sulphide	
Goethite	FeO(OH)	Fe–O	P, S
Goslarite	$ZnSO_4{\cdot}7H_2O$		
Gratonite	$Pb_9As_4S_{16}$		
Gypsum	$CaSO_4{\cdot}2H_2O$		
Hematite	Fe_2O_3	Fe–O	P
Hydromarchite	$Sn_3O_2(OH)_2$		
Hydronium Jarosite	$Fe_3(SO_4)_2(OH)_5{\cdot}2H_2O$	Fe–S–O	S
Illite	$K_{0.5}(Al,Fe,Mg)_3(Si,Al)_4O_{10}(OH)_2$		
Jamesonite	$FePb_4Sb_6S_{14}$		
Jarosite	$KFe_3(SO_4)_2(OH)_6$	Fe–S–O	P, S
Magnetite	Fe_3O_4		
Malachite	$Cu_2(CO_3)(OH)_2$		
Mallardite	$MnSO_4{\cdot}7H_2O$		
Melanterite	$Fe^{2+}SO_4{\cdot}7H_2O$		
Natrojarosite	$NaFe_3(SO_4)_2(OH)_6$	Fe–S–O	S
Parabutlerite	$Fe^{3+}(SO_4)(OH){\cdot}2H_2O$		
Plumbojarosite	$Pb_{1/2}Fe_3(SO_4)_2(OH)_6$	Fe–S–O	P, S
Pyrite	FeS_2	Sulphide	P
Quartz	SiO_2		
Scorodite	$FeAsO_4{\cdot}2H_2O$	Fe–As–O	P
Sphalerite	ZnS	Sulphide	P
Stannite	Cu_2FeSnS_4		
Sulphur	S		
Schwertmannite	$Fe_{16}O_{16}(OH)_{12-10}(SO_4)_{2-3}$	Fe–S–O	S
Symplesite	$Fe_3(AsO_4)_2{\cdot}8H_2O$	Fe–As–O	P
Tenorite	CuO		
Tennantite	$(Cu,Ag,Fe,Zn)_{12}As_4S_{13}$		
Tetrahedrite	$Cu_{12}Sb_4S_{13}$		
Voltaite	$K_2Fe_5^{2+}Fe_4^{3+}(SO_4)_{12}{\cdot}18H_2O$		

Table 2
Trace metal geochemistry of representative Rio Tinto mine-waste, tailings and overbank sediments. All analyses by AAS, except those marked by a '*', which are by XRF (Philips PW1400, Schell, unpublished data); all concentrations in mg/kg; º = samples taken from surface of alluvium and mine-waste and tailings tips; # = samples taken at depth within alluvium and mine-waste and tailings tips; bdl = below detection limit; nd = not determined; nr = not reported; C.O.V. = coefficient of variation, calculated as the standard deviation expressed as a percentage of the mean, values are based on the analysis of 11 sets of triplicate samples; Recovery = percentage of metal extracted by the HNO_3 digestion relative to the total metal content given by the manufacturer, values are based on the analyses of 11 samples of standard sediment reference samples STSD–1 to STSD–4

Sample	Ag	As	Cu	Fe	Mn	Pb	Zn
Mine tailings (purple-red)							
RT3aº	150	5500	4300	27 000	55	2500	1300
RT3b*	nd	2900	1300	nd	nd	31 000	1300
RT3c*	nd	910	100	nd	nd	15 000	nd
Mine-waste							
RT8º	bdl	290	130	20 000	24	1600	59
Mine-waste and tailings							
RT4º	35	380	67	20 000	bdl	6300	34
Fe-rich cement							
RT6º	bdl	230	320	94 000	35	1400	480
Purple-red alluvium (tailings-derived)							
RT26#	15	250	230	47 000	140	2600	260
RT28#	30	620	1500	5300	39	1200	1200
RT31#	16	160	200	35 000	36	7600	60
Pyrite-rich alluvium							
RT1º	bdl	270	340	12 000	38	1400	98
RT2#	bdl	440	420	51 000	64	1600	190
Orange laminated alluvium							
RT24#	bdl	750	84	68 000	26	3100	27
Other alluvium							
RT9º	bdl	430	90	19 000	bdl	870	bdl
RT15#	bdl	460	75	23 000	29	870	26
RT17º	bdl	110	300	40 000	52	1500	120
RT23#	bdl	270	160	37 000	50	1400	65
RT27º	bdl	360	80	35 000	38	660	37
RT30º	bdl	300	130	52 000	86	790	64
RT33º	bdl	474	210	19 000	48	490	120
Detection limits	9.2	6.2	16	57	11	11	21
Precision (C.O.V.%)	20	8	8	8	7	9	7
Accuracy (recovery %)	60	73	86	67	73	68	84
Pleistocene alluvium; Schell et al., 1996	bdl	38	38	37 000	570	24	76
Rio Tinto bottom sediments; Nelson and Lamothe, 1993	nr	< 200–3000	30–1500	2000–100 000	150–300	< 10–2000	< 200–3000
ICRCL threshold trigger concentrations (1990)	–	–	–	–	–	300	1000
Dutch 'A'-values (Anonymous, 1983)	–	29	50	–	–	50	500
'Background' shale and clay (Salomons and Förstner, 1984)	–	–	45	47 200	600	20	95
'Background' soil (Salomons and Förstner, 1984)	–	–	25.8	32 000	760	29.2	59.8
Mineral Precipitates							
MP1	bdl	610	380	56 000	97	16	750
MP2	bdl	500	500	40 000	80	bdl	800
MP3	bdl	300	410	48 000	bdl	13	530

Analar grade (69% v/v) concentrated HNO_3 was added to each sample and left overnight, covered by a watchglass. The mixtures were then boiled, under reflux, for about 8 h and subsequently evaporated to near dryness. After cooling, 10 mL of 0.5% HNO_3 was added to the residues and the samples were gently warmed. The solutions were then filtered into volumetric flasks through Whatman No. 541 filter papers, and rinsed frequently with 0.5% HNO_3. They were then made up to volume using 0.5% HNO_3 and where

necessary, diluted 10, 50, 100 or 500 times by volume. Chemical analysis was carried out by atomic absorption spectrophotometry (Pye Unicam SP9 with air/acetylene flame). Triplicate analyses of selected samples were used to check analytical precision, and accuracy was tested by analysis of standard reference sediments STSD–1 to 4 (Canmet). Working blanks were inserted at a frequency of 10% of the total samples analysed and were generally below detection limits for the metals analysed. Detection limits, precisions and accuracies are shown along with the results in Table 2.

River water anions were analysed by ion chromatography (Dionex–4000i). Cations were analysed by inductively coupled plasma atomic emission spectrometry (ICPAES, VG Elemental, Horizon).

4. Results

4.1. Local field area description and alluvial sediment-borne metal concentrations

The Rio Tinto has a catchment area of 1676 km^2, average annual precipitation of 69 cm a^{-1} and average annual discharge of 1 153 100 m^3 (Garcia-Vargas et al., 1980). The river rises ca. 10 km to the north of the mining area, flows through the major mining area and a large area of slag, mine-waste and tailings tips (which are actively eroded by the river) at Nerva, and continues 80 km to the Atlantic Ocean at Huelva. Conglomerates composed of coarse slag fragments cemented by Fe-rich precipitates occur in the mine-waste tip area, and an abandoned railway track, underlain by slag, bedrock fragments and fine-grained (<2 mm) pyritic waste, follows the Rio Tinto from Nerva to Huelva.

Downstream of the mining area, the Rio Tinto is presently incising into older fluvial deposits, but overbank sediment deposits ranging in thickness from a few cm to several m line the channel banks. These bank sequences reveal at least two cut-and-fill alluvial cycles, the youngest of which is generally less than 100–150 a old. The alluvial mineralogy discussed in this paper relates to the younger cycle which is composed in varying proportions of (1) purple-red alluvium (derived from the purple-red tailings); (2) pyrite-rich alluvium; (3) orange laminated alluvium; and (4) 'other' alluvium, including mixtures of these 3 types, and red, grey and yellow sands and silts.

Concentrations of Ag, As, Cu, Pb and Zn in Rio Tinto mine-waste and tailings tips, and the younger alluvial sediment unit typically exceed values in Pleistocene alluvium by several orders of magnitude (Schell et al., 1996; Table 2). Work is ongoing to establish background values in Holocene alluvium. There is no consistent difference between surface and sub-surface concentrations (Table 2). The contaminant metal values reported in Table 2 are considered to be minimum estimates, since the HNO_3 digestion used for trace element analysis probably does not remove all of the metal from the samples (cf. estimates of accuracy, Table 2). Many of the samples collected for this study exceed Dutch trigger (Anonymous, 1983) and UK MAFF (MAFF, 1993) maximum permissible concentrations for soil, and background values for shale and soil (Salomons and Förstner, 1984). Similar findings were reported by Nelson and Lamothe (1993) for Rio Tinto channel sediment. Generally, the alluvial samples exhibit relatively high contents of Pb and As, moderate contents of Cu and Zn and low contents of Ag (Table 2). The purple-red tailings and alluvium related to these tailings are characterised by the highest concentrations of contaminant metals.

Yellow and white precipitates formed on pyrite-rich mine-waste tips, floodplain sediment surfaces, abandoned railway beds and the vertical surfaces of exposed pyrite-rich alluvial units after rains during the field visits. These precipitates were eroded and washed into the river following renewed rainfall. Contents of As and Cu in the precipitates are comparable to those of the alluvium. Zn contents, however, are generally higher, and Pb contents at least an order of magnitude lower, than alluvial and mine-waste and tailings tip samples (Table 2).

4.2. Mineralogy and chemistry of mine-waste and tailings tips, alluvial sediments and precipitates

The mine-waste and tailings tips, and alluvial sediments are dominated by mixtures of chlorite, feldspar, illite and quartz, as well as contaminant metal-bearing minerals including Fe oxides, oxyhydroxides, jarosite and pyrite (Table 3). The mine-waste tips contain large quantities of pyrite and schist bedrock fragments, and the tailings tips are generally purple-red in colour, and are composed of hematite and jarosite.

The Rio Tinto alluvium is characterised by 4 major groups of contaminant-bearing minerals, including (1) sulphides; (2) Fe–As oxides; (3) Fe oxides/hydroxides/oxyhydroxides; and (4) Fe oxyhydroxysulphates. These have been subdivided into 'primary' and 'secondary' types depending on their mode of occurrence (Table 1). Primary minerals are detrital fragments of the ore-body, gossan and mine waste and tailings tips. Secondary minerals include cements and authigenic overgrowths on the primary grains, and the yellow and white precipitates described above.

Sulphides and Fe–As oxides occur mainly as primary minerals (Table 1), especially in alluvium near the mining areas. Pyrite is the most abundant sulphide, and is often associated with chalcopyrite, arsenopyrite, sphalerite and galena occurring as blebs or crack infill-

Table 3
General mineralogy of Rio Tinto mine and overbank sediments. XXX = abundant; XX = accessory; X = trace

Sample	Chlorite	Feldspar	Ferrihydrite	Goethite	Hematite	Illite	Jarosite	Pyrite	Quartz
Mine tailings									
RT3	X				XXX	XX	XXX	XX	XXX
Mine-waste									
RT8	XX			XX		XX	XXX	XX	XXX
Mine-waste and tailings									
RT4	X				XXX	X	XX		XXX
Fe-rich cement									
RT6	X	X	XX	X		XX	XX	X	XXX
Purple-red alluvium (tailings-derived)									
RT26	XX	X			XX	XX	XXX		XX
RT28	XX	X			XXX	X	XXX		XX
RT31	XX	X			XX	XXX	XXX		XXX
Pyrite-rich alluvium									
RT1								XX	XXX
RT2	XXX				X	XXX	XX	XXX	XX
Orange laminated alluvium									
RT24	XX			X	X	XX	XX	X	XXX
Other alluvium									
RT9				XX					XXX
RT15	XX	X		X		XX	XX		XXX
RT17	XX	XX			X	XX	XX	X	XXX
RT23	X	X			X	XX	X	X	XXX
RT27	X	X		X		X	X		XXX
RT30		XX			XX	XX	XX	X	XX
RT33	XX	X		XX		XX	XX	X	XXX

ings (Fig. 2a). The Fe–As oxides occur as sub- to euhedral grains (Fig. 2b). They display compositions between scorodite and symplesite (Fig. 3, Fe–As–O group), and contain the most As of all the contaminant metal minerals except arsenopyrite, but very little Cu, Pb or Zn.

Both primary and secondary oxides, hydroxides and oxyhydroxides of Fe occur in all types of alluvium throughout the Rio Tinto system. Primary Fe oxides include goethite and hematite in detrital fragments of gossan, and hematite in fragments of the purple-red tailings tip material (Fig. 2d). Secondary oxides include those in Fe-rich cements (Fig. 2c, Fig. 4), and in authigenic overgrowths on quartz and slate grains. XRD analysis suggests that these are mixtures of goethite and possibly ferrihydrite. The primary and secondary Fe oxides/hydroxides/oxyhydroxides generally contain low concentrations of As, Pb and Zn (Fig. 3, Fe–O group; Fig. 4), but some secondary minerals in this group contain some Cu (Fig. 3).

Iron oxyhydroxysulphates are the most common contaminant metal-bearing minerals in the alluvium, and also occur in both primary and secondary forms. In the purple-red tailings tips and related alluvium, honeycomb-like hematite latticeworks are coated by primary Fe oxyhydroxysulphates (Fig. 2d), which have been confirmed by XRD to include both jarosite and plumbojarosite. Elevated Ag values in these and other tip and alluvial types (Table 2), and previous work in the Rio Tinto (Amorós et al., 1981, Dutrizac et al., 1983) suggest that argentojarosite may also be present. SEM–EDX analysis also suggests that a Pb-rich Fe oxyhydroxysulphate mineral, possibly beaverite (Fig. 3) may also be present. Primary Fe oxyhydroxysulphate minerals from the mine/tailings tips and 'other' alluvium are characterised by the highest concentrations of As next to the Fe–As oxides (Fig. 3) and arsenopyrite, and the highest amounts of Pb of all of the contaminant metal-bearing minerals.

Secondary Fe oxyhydroxysulphates occur as overgrowths on pyrite (Fig. 2a) and primary honeycomb hematite-jarosite lattice grains, and in Fe-rich cements (Fig. 4). They include minerals of the jarosite family (e.g., jarosite, plumbojarosite), and possibly beaverite and schwertmannite (see below) (Fig. 3). The secondary Fe oxyhydroxysulphates contain relatively high contents of Pb, though not as high as many of the primary Fe oxyhydroxysulphates. Some of the secondary Fe oxyhydroxysulphate minerals from the purple-red and pyrite-rich alluvium contain relatively high concentrations of Cu and Zn (Fig. 3).

Many of the secondary Fe oxyhydroxysulphates in

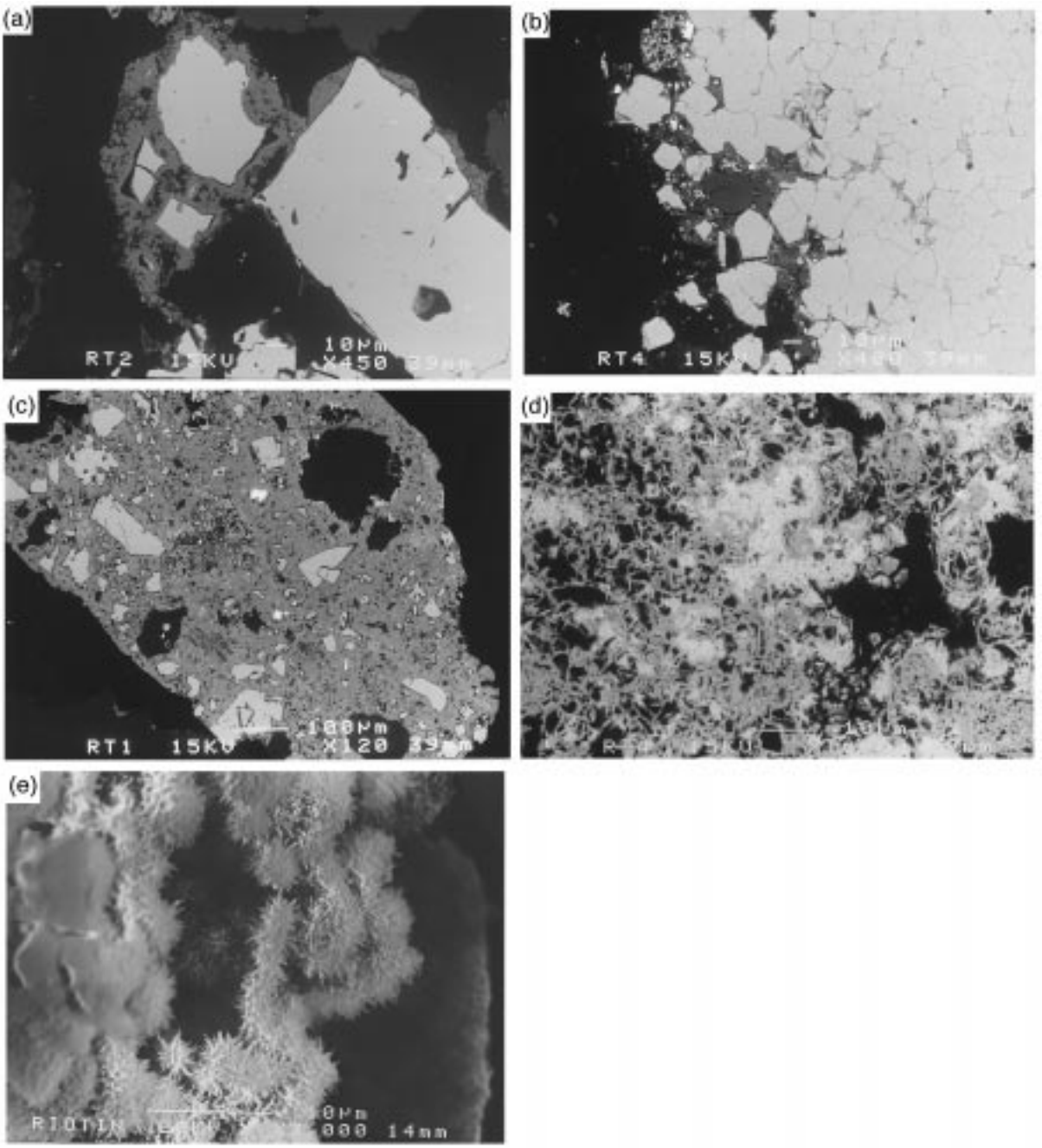

Fig. 2. Back-scattered image SEM photomicrographs. (a) Overgrowths of secondary Pb-bearing Fe oxyhydroxysulphate (grey) on primary pyrite (large white grains). Bright white specks within pyrite are chalcopyrite; (b) Subhedral, interlocking grains of primary Fe–As oxide minerals; (c) primary pyrite grains (bright grey) cemented by complex mixture of baryte (bright white), and secondary Fe oxyhydroxysulphates and oxyhydroxides; (d) Needles of hematite (grey), cemented by Pb-, As-, Cu- and Zn-bearing jarosite (white) in detrital, primary gossan grain. X-ray mapping of this sample indicates that the jarosite contains significant quantities of Pb, As, Cu and Zn; (e) Fe (oxyhydroxy)sulphate crystals from filtered precipitates of Rio Tinto water. These morphologically resemble schwertmannite (cf., Bigham et al., 1994).

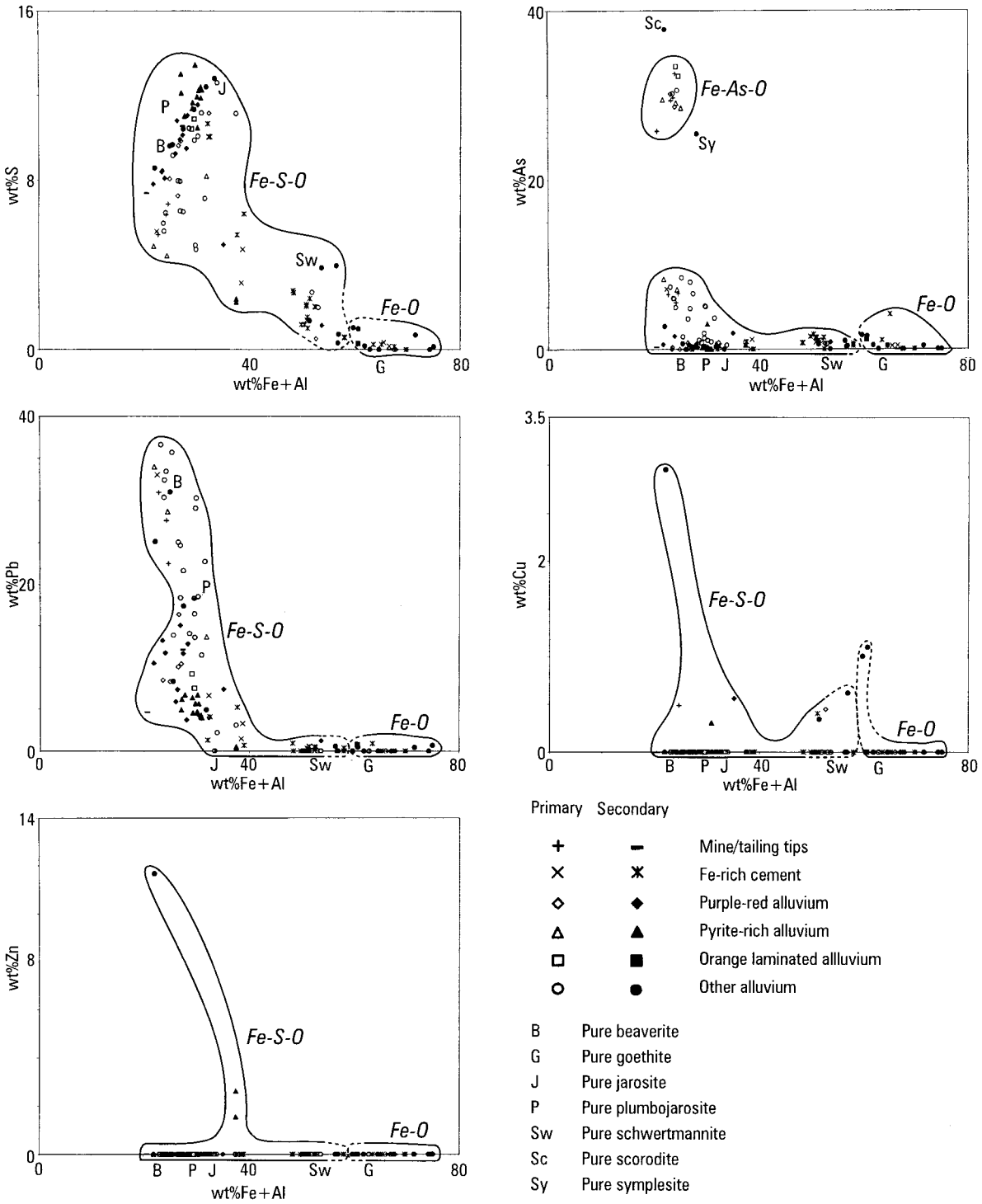

Fig. 3. X–Y plots of Rio Tinto minerals. Fe + Al versus S, As, Pb, Cu and Zn. All values are in wt. %. Fields for Fe–As minerals [Fe–As–O], Fe oxides/hydroxides/oxyhydroxides [Fe–O] and Fe oxyhydroxysulphates [Fe–S–O] are shown. The Fe–As–O group is not shown in the plots for Pb, Cu and Zn because these minerals contain no detectable concentrations of these contaminant metals.

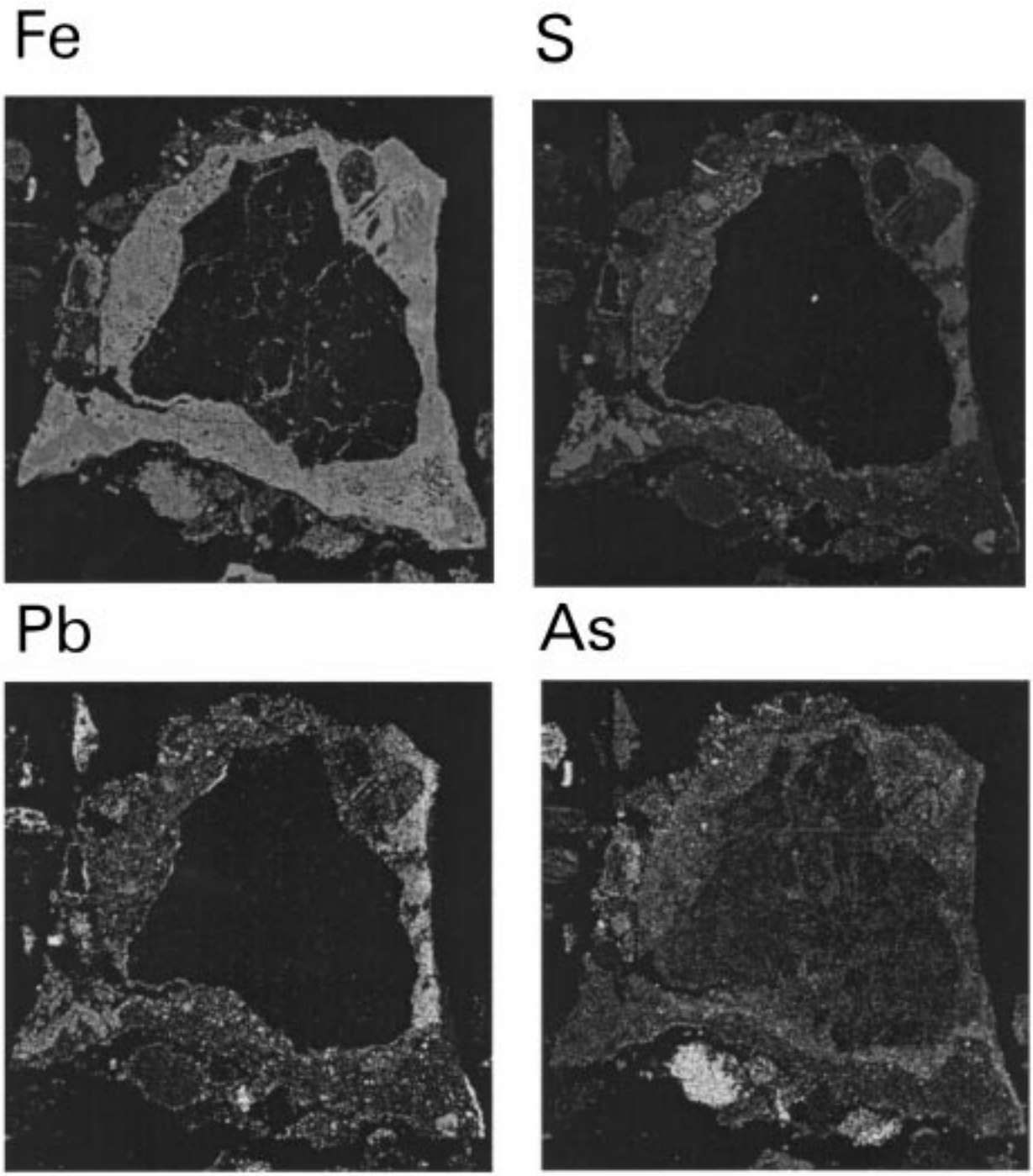

Fig. 4. Electron microprobe X-ray element maps showing complex secondary Fe-rich cement on shale grain (river alluvial sediment sample RT6) (i) Fe; (ii) S; (iii) Pb; (iv) As. Pb, some As, Cu and Zn (not shown) are associated with the Fe–S phase in the cement. Much of the As is associated with the Fe-rich, S-poor portion of the cement.

Table 4
Partial geochemistry of Rio Tinto river and estuary water. All element and anion concentrations in mg/L. bdl = below detection limit; ns = no standard

Sample	River	pH	Conductivity	Temperature	Ag	As	Cu
W1	Rio Tinto	1.8	1500	21	0.03	14	240
W2	Rio Tinto	1.6	1500	20	0.02	11	150
W3	Rio Tinto	1.4	1500	27	0.03	22	210
W4	Rio Tinto	1.9	1500	25	0.01	12	70
W5	Rio Tinto	1.8	1600	26	0.02	25	120
W6	Rio Tinto	1.7	1600	25	0.03	16	170
W7	Rio Tinto	1.5	1500	26	0.01	1.8	44
W8	Rio Tinto	6.0	1300	23	bdl	0.9	24
W9	Tinto Estuary	7.6	1600	26	0.01	0.5	0.05
W10	Upstream tributary	6.4	350	21	bdl	0.2	0.01
W11	Corumbel Reservoir	7.5	490	24	bdl	0.2	bdl
Detection limit					0.005	0.1	0.005
European guideline values					0.01	0.05	ns

Sample	Fe	Pb	Zn	Cl^-	SO_4^{2-}	HSO_4^-
W1	3500	0.8	130	19	14 000	bdl
W2	2400	0.7	110	62	8900	bdl
W3	4300	2.4	420	32	15 000	bdl
W4	2000	1.6	66	21	6900	7
W5	3800	1.7	250	45	13 000	bdl
W6	3700	0.8	310	73	16 000	bdl
W7	630	0.2	100	93	4400	bdl
W8	300	0.1	56	130	2800	bdl
W9	bdl	0.1	0.3	22 000	3400	bdl
W10	1.1	bdl	0.08	6	37	bdl
W11	bdl	bdl	0.04	12	42	bdl
Detection limit	0.1	0.005	0.005	1	1	5
European guideline values	300	0.05	ns	ns	ns	ns

the Fe-rich cements, pyrite-rich, purple-red and 'other' alluvium contain low amounts of S (Fig. 3, Fe–S–O group, right side). These have similar SO_4:Fe + Al ratios to schwertmannite (cf. Bigham et al., 1990), but may also be Fe oxide/hydroxide/oxyhydroxides with adsorbed sulphate (cf. Filipek et al., 1987). Several of these minerals within 'other' alluvium exhibit anomalous amounts of Cu (Fig. 3), but As, Pb and Zn contents are generally low (Fig. 3).

The yellow and white precipitates which form on pyrite-rich mine-waste tips, floodplain sediment surfaces, abandoned railway beds and the vertical surfaces of exposed pyrite-rich alluvial units are also classified as secondary minerals. They are comprised of mixtures of gypsum, alunogen and the Fe oxyhydroxysulphates copiapite, coquimbite, plumbojarosite and hydronium jarosite (see Table 1 for formulas). These precipitates contain moderate to high concentrations of As, Cu and Zn (Table 2).

4.3. River water chemistry and precipitates from river water

Results for Rio Tinto water (samples W1–W9, Table 4) agree with earlier findings of Garcia-Vargas et al. (1980) and López-Archilla et al. (1993), and indicate that, compared to tributary and reservoir water in the area (samples W10, W11, Table 4), the water is acid and carries high amounts of contaminant metal, Fe and SO_4. Concentrations of Cu and Zn exceed those of Pb, As and Ag by at least an order of magnitude. Lead contents gradually decline downstream of the mining area. The other contaminant metal, and Fe contents fluctuate considerably downstream of the mining area, but they all decrease sharply near the estuary (samples W7 and W8, Table 2). Concentrations of contaminant metal, particularly Cu and Zn, are generally higher than those reported for

other acid mine drainage areas (Table 2; e.g., Förstner and Wittman, 1979; Filipek et al., 1987).

As previously shown by López-Archilla et al. (1993), the water pH remains remarkably constant at around 1.7 from the mining area to 60 km downstream (sample W8), where it increases to 6 to 7.6, probably due to the influx of sea water up to the tidal limit. This influx also results in an extremely large increase in Cl^- contents (Table 4).

Filtered precipitates from the river waters are generally bright orange in colour. XRD investigations reveal that they are mixtures of goethite and jarosite. SEM–EDX analysis, however, suggests that there may be another, possibly X-ray amorphous, Fe oxyhydroxysulphate phase present (Fig. 2e), which contains minor amounts of Cu, Pb, S and Zn. This morphologically resembles synthetic schwertmannite (Bigham et al., 1994, Fig. 1), which consists of spherical to ellipsoidal aggregates with needle-like structures radiating from the particle surface to give a 'pin-cushion' morphology.

5. Discussion

5.1. Inferred chemical and mineralogical processes

Since the modes of formation of primary sulphides, Fe–As oxides, Fe oxyhydroxides and oxyhydroxysulphates in the Rio Tinto orebody and gossan have been discussed at length in the literature (e.g., Williams, 1950; Pryor et al., 1972; Amorós et al., 1981; Dutrizac et al., 1983), the following discussion focuses on Rio Tinto secondary minerals in the alluvium. The sulphide assemblage in the Rio Tinto mine-waste tips, railway beds and alluvium is dominated by pyrite which yields acidic weathering products by well-known reactions:

$$FeS_2 + 8H_2O = Fe^{2+} + 2SO_4^{2-} + 16H^+ + 14e^- \quad (1)$$

$$4FeS_2 + 14O_2 + 4H_2O = 4Fe^{2+} + 8H^+ + 8SO_4^{2-} \quad (2)$$

$$FeS_2 + 14Fe^{3+} + 8H_2O = 15Fe^{2+} + 2SO_4^{2-} + 16H^+ \quad (3)$$

The Fe^{2+} produced in reactions such as those of Eqs. (1)–(3) is rapidly oxidised to Fe^{3+} which is strongly hydrolysed to form Fe hydroxide precipitates:

$$Fe^{3+} + 3H_2O = Fe(OH)_3 + 3H^+, \quad (4)$$

and Fe oxyhydroxysulphate precipitates (cf., Brown, 1971; van Breeman and Harmsen, 1975; Bigham et al., 1990; Stahl et al., 1993):

$$3Fe^{3+} + K^+ + 2SO_4^{2-} + 6H_2O = KFe_3(SO_4)_2(OH)_6 + 6H^+ \text{ (Jarosite)} \quad (5)$$

$$16Fe^{3+} + 2SO_4^{2-} + 28H_2O = Fe_{16}O_{16}(OH)_{12}(SO_4)_2 + 44H^+ \text{ (Schwertmannite)} \quad (6)$$

Reactions such as those in Eq. (4) to Eq. (6) may account for secondary Fe minerals in Rio Tinto cements (Fig. 2c, Fig. 3) and grain coatings, and in the filtered water precipitates (Fig. 2e). These occurrences are also consistent with observations of sulphurised soils (Carson et al., 1982) and experimental work (Brown, 1971; van Breeman and Harmsen, 1975; Stahl et al., 1993). Enrichment of contaminant metals in the secondary Fe minerals (Fig. 3, Fig. 4) is consistent with experimental and observational work on Fe oxides/hydroxides/oxyhydroxides (Langmuir and Whittemore, 1971; Benjamin and Leckie, 1981; Nordstrom, 1982; Chapman et al., 1983; Johnson, 1986) and Fe oxyhydroxysulphates (Ivarson et al., 1979; Dutrizac and Kaiman, 1976; Dutrizac, 1983; Dutrizac and Jambor, 1987; Webster et al., 1998), which suggests that the contaminant metals may be adsorbed onto or co-precipitated with these minerals.

The apparent greater affinity of the Rio Tinto Fe oxyhydroxysulphates relative to Fe oxides/hydroxides/oxyhydroxides for contaminant metals might be explained by experimental studies. Brady et al. (1986) suggested that concentrations of SO_4^{2-} as low as 250 mg/L may suppress the formation of Fe hydroxides such as ferrihydrite. This would allow Fe oxyhydroxysulphates to precipitate first and preferentially scavenge contaminant metals. Webster et al. (1998) suggested that SO_4^{2-} positively influences Cu, Pb and Zn adsorption onto Fe oxides and oxyhydroxysulphates by the formation of ternary complexes between the mineral surface, SO_4^{2-} and the metal ion. A similar mechanism was also proposed by Ali and Dzombak (1996) for enhanced Cu adsorption onto goethite in the presence of SO_4^{2-}.

The yellow-white minerals on pyrite-rich alluvium and railway beds, and the Fe oxyhydroxysulphates on pyrite grains within other types of alluvium (cf., Fig. 2a; Table 3) may all form as a result of precipitation of Fe^{2+}, Fe^{3+} and SO_4^{2-} ions which have been provided by pyrite oxidation (Eqs. (1)–(3)) and water, e.g.:

$$Fe^{2+} + 4Fe^{3+} + 6SO_4^{2-} + 22H_2O = Fe_5(SO_4)_6(OH)_2 \cdot 20H_2O + 2H^+ \text{ (Copiapite)} \quad (7)$$

$$2Fe^{3+} + 3SO_4^{2-} + 9H_2O = Fe_2(SO_4)_3 \cdot 9H_2O \text{ (Coquimbite)} \quad (8)$$

In the Rio Tinto alluvium, this occurs (i) directly on the pyrite grain surface (Fig. 2a; cf., Huggins et al., 1983); (ii) by precipitation of evaporating acid pore water, as in abandoned Rio Tinto mine shafts (García, 1996) and other acid drainage areas (e.g., Nordstrom et al., 1979); or (iii) as dehydration products of other hydrated Fe sulphate minerals (cf., Ehlers and Stiles, 1965). These minerals also appear to scavenge contaminant metals (Fig. 2a; Table 2).

Alternatively, the Rio Tinto secondary goethites and jarosites may have formed as a result of the recrystallisation of minerals such as ferrihydrite or schwertmannite (cf., Bigham et al., 1990; Webster et al., 1998), as discussed in the next section.

The significant decreases in Fe and SO_4^{2-} downstream river water concentrations (Table 4) suggest that precipitation of Fe− and SO_4-bearing minerals is taking place. Concomitant declines in aqueous contaminant metal contents suggests that the metals are sorbed or co-precipitated by these minerals. This appears to be at least partly governed by pH, but some of the declines in downstream element contents (e.g., As, Cu, Fe) are recorded in acid water (sample W7, pH 1.5), suggesting that another, at present unknown, mechanism may be responsible.

5.2. Mobility of contaminant metal-bearing minerals in alluvium

The relative mobility of the contaminant metals in the alluvium can be assessed by examining both water (Table 4) and mineralogical data (Fig. 3). Low concentrations of Pb and As relative to Cu and Zn in Rio Tinto water imply that Pb and As are less readily mobilised from the alluvium, mine tailings and waste tips. This is supported by depletion of Pb and As in secondary relative to primary Fe oxyhydroxysulphates, suggesting that the primary oxyhydroxysulphates may have greater binding strength for these contaminant metals. Enrichment of As, Cu, Pb and Zn in secondary relative to primary Fe oxide/hydroxide/oxyhydroxide minerals, and of Cu and Zn in secondary relative to primary oxyhydroxysulphate minerals (Fig. 3), demonstrates that some of the aqueous contaminant metal (which was probably leached from primary minerals) is incorporated in the secondary minerals.

Mobilisation of As, Cu, Zn, and to a lesser extent, Pb, may explain the contaminant metal chemistry of the secondary yellow-white precipitates (MP samples, Table 2). These precipitates are destroyed and probably dissolved following periods of high rainfall, probably re-releasing the As, Cu, Zn and Pb. Such 'flush-out' events have been described in acid mine drainage systems elsewhere (e.g., Alpers et al., 1991) where they produce a rapid increase in aqueous metal concentrations and acidity.

Primary contaminant metal-bearing minerals in the Rio Tinto alluvium, including hematite, goethite, jarosite and plumbojarosite, and the Fe–As minerals (possibly scorodite), generally have very low solubility products (Langmuir and Whittemore, 1971; Robins, 1990; Doyle et al., 1994; Baron and Palmer, 1996) and are likely to be more stable than many of the poorly crystalline, secondary Fe oxides/hydroxides/oxyhydroxides and oxyhydroxysulphates. Experimental data suggests, however, that ferrihydrite and schwertmannite over time recrystallise to more stable phases such as goethite and jarosite (Bigham et al., 1990; Webster et al., 1998), but it is uncertain as to how this transformation affects contaminant metal mobility.

Some of the relatively insoluble alluvial minerals may become unstable, however, if environmental conditions change or if remedial measures such as raising river pH are implemented. Jarosite can transform to Fe oxides or hydroxides by hydrolysis or simple dissolution and reprecipitation, although this is likely to be a slow process (van Breeman and Harmsen, 1975; Brady et al., 1986). Baron and Palmer (1996) suggested that the transformation of jarosite to ferric oxyhydroxide occurs above pH 5.89, but the mechanism of redistribution of associated contaminant metals is not known. Dissolved Fe^{2+}, which could be generated from reactions Eq. (1) to Eq. (3), is known to catalyse the dissolution of crystalline Fe oxides (Fischer, 1972; El-Desoky, 1989) and jarosite (El-Desoky, 1989). Despite this, raising river water pH would likely result in the precipitation of Fe oxides/hydroxides/oxyhydroxides and oxyhydroxysulphates, which would scavenge or co-precipitate contaminant metals (e.g., Benjamin and Leckie, 1981). This appears to occur down-river in the Rio Tinto (see above), and has a positive effect on water quality (Table 4), but a potentially negative effect on sediment quality.

6. Conclusions

1. Rio Tinto alluvium is contaminated with Ag, As, Cu, Pb and Zn. The major mineralogical hosts of these elements are sulphides, Fe-As oxides, Fe oxides/hydroxides/oxyhydroxides, and Fe oxyhydroxysulphates.
2. These alluvial minerals are both 'primary' detrital remnants of mine-waste and tailings tips, and 'secondary' products of a series of oxidation, dissolution and precipitation reactions.
3. Cu and Zn appear to be more mobile than Pb and As in the Rio Tinto alluvium. Although many of the Rio Tinto Fe oxides/hydroxides (hematite, goethite) and oxyhydroxysulphates (jarosite) are

insoluble, some which are inferred to occur (ferrihydrite, schwertmannite) are less stable. Erosion of contaminant metal-rich purple-red tailings, erosion and oxidation of pyrite-rich mine-waste tips and alluvium, dissolution of Fe sulphate salts (e.g., copiapite, coquimbite) and oxidation of pyrite from railway beds will probably continue to contribute to metal pollution in the Rio Tinto.

4. Raising river pH would probably would have positive effects on water quality by causing precipitation of minerals which sorb or co-precipitate contaminant metals. This already appears to occur near the Tinto estuary. This action, however, may also lead to de-stabilisation of contaminant metal-bearing minerals such as jarosite, possibly re-releasing metals back to the aqueous system.

Acknowledgements

The authors would like to thank NERC and the Universities of Manchester and Leeds for funding. C. Schell is in receipt of a postgraduate studentship from the School of Geography, University of Leeds. We are grateful to D. Plant and T. Hopkins for assistance with the SEM and microprobe, P. Lythgoe for help with ICP–AES analyses, A. Brewsher for ion chromatograph analyses, A. French and L. Wright for preparation of diagrams, M. Fey and J. Webster for helpful discussions and advice, and S. Black for reading an early version of the manuscript. J. Ridgway and one anonymous reviewer are thanked for their constructive comments on and criticisms of, the manuscript.

References

Ali, M.A., Dzombak, D.A., 1996. Interactions of copper, organic acids, and sulfate in goethite suspensions. Geochim. Cosmochim. Acta 60, 5045–5053.

Alpers, C.N., Maenz, C., Nordstrom, D.K., Erd, R.C., Thompson, J., 1991. Storage of metals and acidity by iron-sulfate minerals associated with extremely acidic mine waters, Iron Mountain, California (abstract). Geol. Soc. Am. Ann. Mtg, A382. San Diego.

Amorós, J.L., Lunar, R., Tavira, P., 1981. Jarosite: a silver bearing mineral of the gossan of Rio Tinto (Huelva) and la Union (Cartagena Spain). Mineral. Deposita 16, 205–213.

Anonymous, 1983. Leidraad Bodemsanering. Dutch Ministry of Housing, Physical Planning and Environment. Leidschendam, The Netherlands.

Badham, J.P.N., 1982. Further data on the formation of ores at Rio Tinto Spain. Trans. Inst. Min. Metall. (Sect. B: Appl. Earth Sci.) 91, B26–B32.

Baron, D., Palmer, C.D., 1996. Solubility of jarosite at 4–35°C. Geochim. Cosmochim. Acta 60, 185–195.

Benjamin, M.M., Leckie, J.O., 1981. Multiple-site adsorption of Cd, Cu, Zn, and Pb on amorphous iron oxyhydroxide. J. Colloid Interface Sci. 79, 209–221.

Bigham, J.M., Schwertmann, U., Carlson, L., Murad, E., 1990. A poorly crystallised oxyhydroxysulfate of iron formed by bacterial oxidation of Fe(II) in acid mine waters. Geochim. Cosmochim. Acta 54, 2743–2758.

Bigham, J.M., Carlson, L., Murad, E., 1994. Schwertmannite, a new iron oxyhydroxysulphate from Pyhäsalmi, Finland and other localities. Min. Mag. 58, 641–648.

Boult, S., Collins, D.N., White, K.N., Curtis, C.D., 1994. Metal transport in stream polluted by acid mine drainage; the Afon Goch, Anglesey, UK. Env. Pollut. 84, 279–284.

Boyle, E.A., Chapnick, S.D., Bai, X.X., Spivak, A.J., 1988. Trace metal enrichments in the Mediterranean Sea. Earth Planet. Sci. Lett. 74, 405–550.

Brady, K.S., Birham, J.M., Jaynes, W.F., Logan, T.J., 1986. Influence of sulfate on Fe-oxide formation: comparison with a stream receiving acid mine drainage. Clays Clay Miner. 34, 266–274.

Brown, J.B., 1971. Jarosite-goethite stabilities at 25°C 1 atm. Mineral. Deposita 6, 245–252.

Calderón, S., 1910. Los Minerales de España. Eduardo Aria, Madrid.

Carson, C.D., Fanning, D.S., Dixon, J.B., 1982. Altisols and Ultisols with acid sulfate weathering features in Texas. In: Acid Sulfate Weathering, pp. 109–126. Soil Sci. Soc. Am.

Chapman, B.M., Jones, P.R., Jung, R.F., 1983. Processes controlling metal ion attenuation in acid mine drainage streams. Geochim. Cosmochim. Acta. 47, 1957–1973.

Davis, A., Drexler, J.W., Ruby, M.V., Nicholson, A., 1993. Micromineralogy of mine waste in relation to lead bioavailability. Environ. Sci. Technol. 27, 1415–1425.

Doyle, T.A., Davis, A., Runnells, D.D., 1994. Predicting the environmental stability of treated copper smelter flue dust. Appl. Geochem. 9, 337–350.

Dutrizac, J.E., 1983. Factors affecting alkali jarosite precipitation. Metall. Trans. B 14B, 531–539.

Dutrizac, J.E., Jambor, J.L., 1987. Behaviour of cesium and lithium during the precipitation of jarosite-type compounds. Hydrometallurgy 17, 251–265.

Dutrizac, J.E., Kaiman, S., 1976. Synthesis and properties of jarosite-type compounds. Can. Miner. 14, 151–158.

Dutrizac, J.E., Jambor, J.L., O'Reilly, J.B., 1983. Man's first use of jarosite: the pre-Roman mining-metallurgical operations at Rio Tinto Spain. Can. Inst. Min. Bull. 76, 78–82.

Ehlers, E.G., Stiles, D.V., 1965. Melanterite-rozenite equilibrium. Am. Miner. 50, 1457–1461.

Elbaz-Poulichet, F., Leblanc, M., 1996. Transfert de métaux d-une province minière à l'océan par les fleuves acides (Rio Tinto, Espagne). Comptes-Rendus de l'Académie des Sciences de Paris 322 (IIa), 1047–1052.

El-Desoky, M.A., 1989. Iron 'oxide' forms and heavy metal transformations in Sulfaquepts in Baltimore Harbor dredged material. Ph.D. thesis, Univ. of Maryland.

Fischer, W.R., 1972. Die Wirkung von zweiwertigem Eisen auf Lösung und Umwandlung von Eisen(III)-hydroxiden. In: Schlichting, E., Schwertmann, U. (Eds.), Pseudogley and Gley. Verlag Chemie, Weinheim, pp. 37–44.

Filipek, L.H., Nordstrom, D.K., Ficklin, W.H., 1987. Interaction of acid mine drainage with waters and sediments of West Squaw Creek in the West Shasta mining district, California. Environ. Sci. Technol. 21, 388–396.

Förstner, U., Wittman, G., 1979. Metal Pollution in the Aquatic Environment. Springer, Berlin.

Fuge, R., Pearce, F.M., Pearce, N.G., Perkins, W.T., 1993. Geochemistry of Cd in the secondary environment near abandoned metalliferous mines, Wales. Appl. Geochem. Suppl. 2, 29–35.

Galan and Mirete, 1979. Introducion a los Minerales de España. IGME Division de Investigaciones Mineras Madrid.

García, G.G., 1996. The Río Tinto Mines Huelva Spain. Mineral. Record 27, 275–285.

Garcia-Vargas, M., Cordon, F., Guerrero, M.A., Coy III, R., 1979. Evaluacion preliminar de la contaminacion por metales pesados en el Estuario del Rio Tinto. Tecnia Investigacion Tratamiento Medio Ambiente 1, 59–68.

Garcia-Vargas, M., Ruiz-Abrio, M.T., Guerrero, M.A., 1980. Determinación de metales pesados por espectroscopia de absorción atómica en la cuenca del río Tinto. Tecnica Investigacion Tratamiento Medio Ambiente 2, 12–24.

Harrison, R.M., Laxen, D.P.H., 1981. Lead Pollution—Causes and Control. Cambridge University Press, Cambridge.

Harvey, C.E., 1981. The Rio Tinto Company: an economic history of a leading international mining concern, 1873-1954. A. Hodge, Penzance.

Huggins, F.E., Huffman, G.P., Lin, M.C., 1983. Observations of low-temperature oxidation of minerals in bituminous coals. Int. J. Coal Geol. 3, 157–182.

Ivarson, K.C., Ross, G.J., Mills, N.M., 1979. The microbiological formation of basic ferric sulfates. II. Crystallization in the presence of potassium ammonium and sodium salts. J. Soil Sci. Soc. Am. 43, 908–912.

Johnson, C.A., 1986. The regulation of trace elements concentrations in river and estuarine waters contaminated with acid mine drainage. Geochim. Cosmochim. Acta 50, 2433–2438.

Jones, G.B.D., 1982. Spring of sweet water marks Rio Tinto's first mining camp. J. Roman Studies, 146–165.

Langmuir, D., Whittemore, D.O., 1971. Variations in the stability of ferric oxides. In: Hem, J.D. (Ed.) Nonequilibrium Systems in Natural Water Chemistry (special issue). Advances in Chemistry Series No. 106.

Leblanc, M., Benothman, D., Elbaz-Poulichet, F., Luck, J.M., Carjaval, D., Gonzalez-Martinez, A.J., Grande-Gil, J.A., Ruiz de Almodovar, G., Saez-Ramos, R., 1995. Rio Tinto (Spain), an acidic river from the oldest and the most important mining area of Western Europe: Preliminary data on metal fluxes. In: Pasava, J., et al. (Ed.), Mineral deposits: from their origin to their environmental impacts. Balkema, Rotterdam, pp. 669–670.

López-Archilla, A.I., Marín, I., Amils, R., 1993. Bioleaching and interrelated acidophilic microorganisms from Río Tinto, Spain. Geomicrobiol. J. 11, 223–233.

Macklin, M.G., 1996. Fluxes and storage of sediment-associated heavy metals in floodplain systems: assessment and river basin management issues at a time of rapid environmental change. In: Anderson, M.G., Walling, D.E., Bates, P.D. (Eds.), Floodplain Processes. John Wiley and Sons, Chichester, pp. 441–460.

Ministry of Agriculture, Fisheries and Food (MAFF), 1993. Code of good agricultural practice for the protection of soil. Welsh Office Agriculture Department.

Morral, F.M., 1990. A mini-history of Rio Tinto. Can. Min. Metall. Bull. 83, 150–154.

Munha, J., Barriga, F.J.A.S., Kerrich, R., 1986. High ^{18}O-forming fluids in volcanic-hosted base metal massive sulfide deposits: Geologic, $^{18}O/^{16}O$, and D/H evidence from the Iberian pyrite belt; Crandon, Wisconsin, and Blue Hill, Maine. Econ. Geol. 81, 530–552.

Muñoz, F.R., González-Regalado, M.L., Flores, J.B., Morales, J.A., 1997. The response of ostracod assemblages to recent pollution and sedimentary processes in the Huelva Estuary, SW Spain. Sci. Total Environ. 207, 91–103.

Nelson, C.H., Lamothe, P.J., 1993. Heavy metal anomalies in the Tinto and Odiel River and Estuary System, Spain. Estuaries 16, 496–511.

Nordstrom, D.K., 1977. Hydrogeochemical and microbiological factors affecting the heavy metal chemistry of an acid mine drainage system. Ph.D. thesis, Stanford Univ.

Nordstrom, D.K., 1982. Aqueous pyrite oxidation and the consequent formation of secondary minerals. Acid Sulphate Weathering. Soil Sci. Soc. Am, 37–56.

Nordstrom, D.K., Jenne, F.A., Ball, J.W., 1979. Redox equilibria of iron in acid mine waters. Am. Chem. Soc. Symp. Ser. 93 (3), 51–79.

Pinedo, V.I., 1963. Piritas de Huelva: su historia, minería y aprovechamiento. Ed. Sucesores de Rivadenegra, Madrid.

Pryor, R.N., Rhoden, M.N., Villalon, M., 1972. Sampling of Cerro Colorado Rio-Tinto, Spain. Trans. Inst. Min. Metall. 81, A143–A159.

Robins, R.G., 1990. The stability and solubility of ferric arsenate: an update. Paper presented at The Metallurgical Society annual mtg., Feb. 18–22, Anaheim CA. The Metallurgical Society, Warrendale, PA., USA.

Ruby, M.V., Davis, A., Nicholson, A., 1994. In situ formation of lead phosphates in soils as a method to immobilize lead. Environ. Sci. Technol. 28, 646–654.

Salomons, W., Förstner, U., 1984. Metals in the Hydrocycle. Springer, Berlin.

Schell, C., Macklin, M.G., Hudson-Edwards, K.A., 1996. Flood dispersal and alluvial storage of heavy metals in an acid ephemeral river: Rio Tinto, Huelva, SW Spain. Proc. Fourth Int. Symp. Geochem. Earth's Surface, 475–479. Ilkley, UK, 21–25 July 1996.

Schermerhorn, L.J.G., 1982. Framework and evolution of Hercynian mineralization in the Iberian Meseta. Comunicacione Geologico Iceo Portugal 1, 91–140.

Stahl, R.S., Fanning, D.S., James, B.R., 1993. Goethite and jarosite precipitation from ferrous sulfate solutions. Soil Sci. Soc. Am. J. 57, 280–282.

Strauss, G.K., Madel, J., Alonso, F.F., 1977. Exploration practice for strata-bound volcanogenic sulphide deposits in the Spanish-Portuguese pyrite belt. In: Klemm, D.D., Scheinder, H.-J. (Eds.), Time and Strata-bound ore deposits. Springer-Verlag, Berlin, pp. 55–93.

van Breeman, N., Harmsen, K., 1975. Translocation of iron in acid sulfate soils: I. Soil morphology and the chemistry

and mineralogy of iron in a chronosequence of acid sulfate soils. Soil Sci. Soc. Am. Proc. 39, 1140–1147.

van Geen, G., Boyle, E.A., 1990. Variability of trace metal fluxes through the Strait of Gibraltar. Palaeogeography, Palaeoclimatology, Palaeoecology 89, 65–79.

van Geen, G., Boyle, E.A., Rosener, P., 1988. Entrainment of trace-metal-enriched Atlantic-shelf water in the inflow to the Mediterranean Sea. Nature 331, 423–426.

van Geen, G., Boyle, E.A., Martin, J.M., 1990. Trace metal enrichments in coastal waters of the Iberian peninsula. EOS (Trans. Am. Geophys. Union) 71, 89.

van Geen, G., Boyle, E.A., Moore, W.S., 1991. Trace metal enrichments in the waters of the Gulf of Cadiz. Geochim. Cosmochim. Acta 55, 2173–2191.

van Geen, A., Adkins, J.F., Boyle, E.A., Nelson, C.H., Palanques, A., 1997. A 120 a record of widespread contamination from mining of the Iberian pyrite belt. Geology 25, 291–294.

Webster, J.G., Swedlund, P.J., Webster, K.S., 1998. Trace metal adsorption onto acid mine drainage Fe (III) oxyhydroxysulphate. Environ. Sci. Technol. 32, 1361–1368.

Welty, A.T., Davis, R., Ryan, J.G., 1995. 5000 years of pollution in the Rio Tinto estuary, south-western Spain. Abstr. Prog. Geol. Soc. America 27, A86.

Williams, D., 1934. The geology of the Rio Tinto mines, Spain. Trans. Inst. Min. Metall. 43, 594–640.

Williams, D., 1950. Gossanized breccia-ores jarosites and jaspers at Rio Tinto, Spain. Inst. Min. Metal. Bull. 526, 1–12.

Williams, D., Stanton, R.L., Rambaud, F., 1975. The Planes-San Antonio pyritic deposit of Rio Tinto Spain: Its nature environment and genesis. Trans. Inst. Min. Metall. (Sect. B: Appl. Earth Sci.) 84, B73–B82.

Wilson, A.J., 1981. Archaeologists find 'missing link' in Rio Tinto mining history. Queensland Gov. Min. J. 82, 32–33.